

In-plane and out-of-plane behavior of confined masonry walls for various tothing and openings details and prediction of their strength and stiffness

Vaibhav Singhal[‡] and Durgesh C. Rai^{*†}

Department of Civil Engineering, Indian Institute of Technology Kanpur, Kanpur, India

SUMMARY

Eight half-scale brick masonry walls were tested to study two important aspects of confined masonry (CM) walls related to its seismic behavior under in-plane and out-of-plane loads. Four solid wall specimens tested to investigate the role of type of interface between the masonry and tie-columns, such as tothing varying from none to every course. The other four specimens with openings were tested to study the effectiveness of various strengthening options around opening to mitigate their negative influence. In the set of four walls, one wall was infilled frame while the other three were CM walls of different configurations. The experimental results were further used to determine the accuracy of various existing models in predicting the in-plane response quantities of CM walls.

Confined masonry walls maintained structural integrity even when severely damaged and performed much better than infill frames. No significant effect of tothing details was noticed although tothing at every brick course was preferred for better post-peak response. For perforated walls, provision of vertical elements along with continuous horizontal bands around openings was more effective in improving the overall response. Several empirical and semi-empirical equations are available to estimate the lateral strength and stiffness of CM walls, but those including the contribution of longitudinal reinforcement in tie-columns provided better predictions. The available equations along with reduction factors proposed for infills could not provide good estimates of strength and stiffness for perforated CM walls. However, recently proposed relations correlating strength/stiffness with the degree of confinement provided reasonable predictions for all wall specimens. Copyright © 2016 John Wiley & Sons, Ltd.

Received 20 April 2015; Revised 14 March 2016; Accepted 9 June 2016

KEY WORDS: confined masonry; seismic performance; lateral strength and stiffness; in-plane response; out-of-plane response

1. INTRODUCTION

The confined masonry (CM) structure consists of load bearing walls strengthened with nominally reinforced concrete elements at the perimeter and other key locations, namely tie-beams and tie-columns. The CM is considerably different from infilled masonry RC frames with respect to (i) construction methodology, as a masonry wall is laid before the columns, and (ii) load transfer mechanism under gravity and lateral load. CM construction has evolved based on its satisfactory performance in past earthquakes [1]. It was observed that CM panels provide fair amount of in-plane shear capacity and ductility under seismic loads, and its behavior can be significantly affected by wall-to-tie-column interface, detailing of confining members and presence of openings. Recent experimental studies have observed that the wall-to-frame connection details play a crucial role in

*Correspondence to: Durgesh C Rai, Department of Civil Engineering, Indian Institute of Technology Kanpur, Kalyanpur, Kanpur, Uttar Pradesh 208016, India.

[†]E-mail: dcrail@iitk.ac.in

[‡]Department of Civil and Environmental Engineering, Indian Institute of Technology Patna, Bihta, India

the in-plane and out-of-plane behavior of masonry panels [2]. Moreover, according to the reconnaissance reports of several past earthquake and research evidences, openings have negative influence upon seismic resistance of CM walls [3, 4]. To compensate for deficiencies due to presence of openings, confinement should be provided on all sides of opening. Guidelines for the suitable confinement around the door and window openings are provided by several national standards and technical manuals [5–8]; however, the efficacy of these confining schemes is still not well known.

In addition, the out-of-plane load-carrying capacity of the masonry panels may be substantially weakened after being damaged, endangering their overall safety and stability. Earlier experimental studies on masonry infill frames concluded that the prior in-plane damage could significantly reduce the out-of-plane capacity of infill panels [9–11]. However, similar studies on the bidirectional response of CM walls have not been conducted, and it is not known which factors play dominant role in the overall behavior of CM walls during earthquakes. The present study is an extension of research on CM walls, and it will evaluate the effect of wall-to-tie-column connection and presence of openings on the bidirectional behavior of CM walls.

An analytical study was also performed with an objective to evaluate the existing predictive relations for strength and stiffness of CM walls with and without openings. Many in-plane strength and stiffness predictive equations are available in the literature for solid CM walls, but similar equations for estimating their strength and stiffness with openings are scarce. These analytical equations are either highly influenced by the formulas originally developed for unreinforced and reinforced masonry walls or are based on the limited number of laboratory tests [12, 13]. This paper will provide a repository of various proposed analytical relations to evaluate the in-plane strength and stiffness of CM walls, and their accuracy will be judged by comparing the predicted values with experimental results of the present study. *In lieu* of scarcity of analytical methods to quantify the negative influence of openings on the in-plane response of CM walls, the suitability of various available reduction factors originally proposed for masonry infilled RC frames is also reviewed.

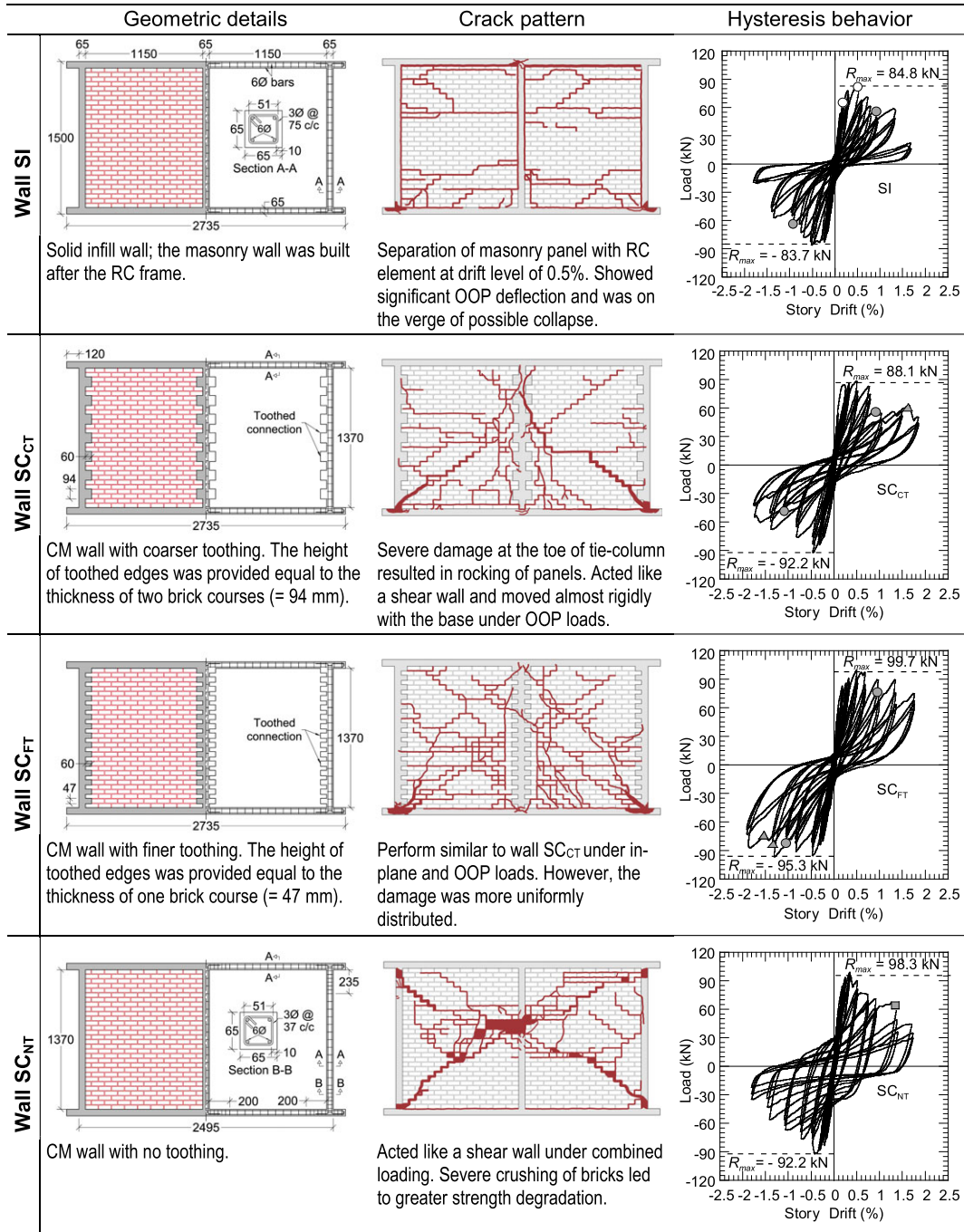
2. EXPERIMENTAL PROGRAM

2.1. Specimen details

The test matrix involved eight half-scaled wall specimens, having dimensions of 2.5-m long by 1.5-m high and 60-mm thick as shown in Figures 1 and 2. The cross-section and reinforcement details were obtained by following the requirements for CM walls from Mexican code (NTC-M, 2004). These figures also summarize key observation and hysteresis behavior of all wall specimens. Two specimens were regular masonry infilled RC frame in which the masonry wall was built after the RC frame. In other six specimens, the confining (frame) elements were constructed after the masonry wall. In this experimental study, the only difference between the infill wall and CM wall is the method of construction whereas the dimensions of confining frames were kept same. Four solid wall specimens were prepared to study the influence of type of the interface present at the wall edge and column, such as tothing (Figure 1). To evaluate the effect of density of the tothing, three different variations were examined in CM wall specimens. Another four specimens had openings for door and windows to evaluate the efficiency of different arrangements of horizontal and vertical members around openings (Figure 2).

Walls are designated by alphanumeric symbol as SI, SC_{CT}, SC_{FT}, SC_{NT}, SI-O_{2WA}, SC-O_{2WB}, SC-O_{2WC}, and SC-O_{DWB}, where letters I and C denote infilled and CM wall, respectively, and O signifies the wall with openings. The subscripts CT, FT, and NT represent coarser, finer, and no tothing present in solid walls, respectively. Subscripts W and D represent type of opening, that is, window and door opening, respectively, and numeric symbol corresponds to number of window openings. The subscripts A, B, and C signify the type of confinement scheme used to enclose the opening as shown in Figure 2.

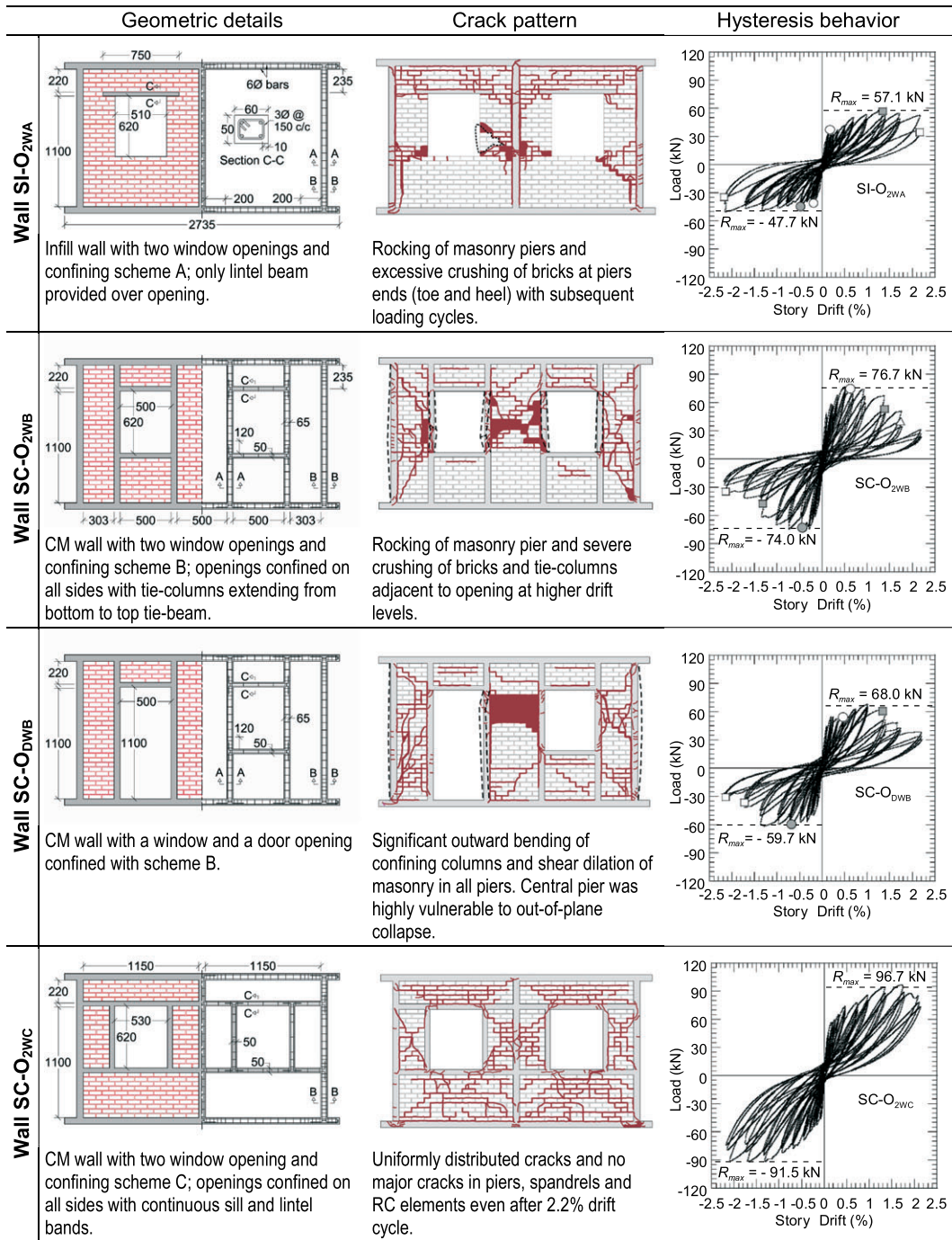
Specially made half-scaled burnt clay bricks and a lime-cement mortar mix of 1:1:6 proportion (cement:lime:sand) was used for masonry panels. The physical and mechanical properties of these



- Separation at wall-to-column connection
- △ Fracturing of longitudinal rebar
- Rocking of masonry panel or pier
- Crushing of bricks
- ▲ Buckling of longitudinal rebar
- Failure of masonry pier

Figure 1. Details of solid walls along with summary of failure pattern and hysteresis behavior. OOP, out-of-plane, CM, confined masonry.

chosen half-scale brick masonry correlated well with that of full-scale bricks [14]. Micro-concrete was used in RC members of all specimens. To monitor whether the green concrete is completely filled in toothed edges, transparent perspex sheet was used as a formwork for tie-column. With the designed concrete mix, it was observed that the toothed edges were completely filled with concrete, and good consolidated hardened concrete was observed after removing the formwork. The average reference



- Separation at wall-to-column connection ● Rocking of masonry panel or pier ▲ Buckling of longitudinal rebar
- △ Fracturing of longitudinal rebar ■ Crushing of bricks □ Failure of masonry pier

Figure 2. Details of perforated walls along with summary of failure pattern and hysteresis behavior. CM, confined masonry.

properties of material, masonry compressive strength $f_m^{c'}$, modulus of masonry E_m , and compressive strength of concrete $f_c^{c'}$ are listed in Table I. The steel wires of 6 and 3 mm diameter were used as longitudinal and transverse reinforcement in RC members, respectively. The yield strength of 6 and 3 mm diameter bars was 426 and 623 MPa, respectively.

Table I. Average properties of materials and summary of various response parameters.

Wall	f_m^c (MPa)	E_m (MPa)	f_c^c (MPa)	Ultimate load, R_{max} (kN)	Displacement at peak load (mm)*	Cumul. energy dissipated (kN m)	Strength degradation
SI	10.3	2960	30.1	84.2	7.2 (0.48)	8.1	0.24
SC _{CT}	8.2	3165	43.6	90.1	7.1 (0.47)	11.8	0.58
SC _{FT}	9.4	3353	40.7	97.5	7.2 (0.48)	12.8	0.80
SC _{NT}	8.8	3845	33.1	95.2	5.8 (0.39)	18.2	0.41
SI-O _{2WA}	7.5	2628	30.6	52.4	20.2 (1.35)	7.9	0.88
SC-O _{2WB}	7.8	2854	30.3	75.3	6.9 (0.46)	11.5	0.44
SC-O _{DWB}	8.5	3927	34.1	63.8	14.7 (0.98)	10.2	0.53
SC-O _{2WC}	7.9	3026	30.3	94.1	25.4 (1.69)	12.0	0.93

*Figures in parentheses, (), indicate the drift in percent (%).

2.2. Test procedure and loading history

The testing method involved successive applications of out-of-plane and in-plane loading [11]. The test setup for the out-of-plane and in-plane loading are shown in Figure 3. An overburden pressure of 0.10 MPa was applied on wall specimens to simulate the loads from upper story walls (ignoring floor load) of a typical three story masonry building. A low overburden was applied to the specimen because of limitation of the test setup and payload capacity of the shake table. The vertical pressure was applied by means of post-tensioned cables (flexible wire) using turn buckle arrangement at four predefined positions along the length of the specimen. For simulation of out-of-plane forces, the artificial mass in form of lead blocks as required by dynamic similitude relations were attached to the walls in a regular grid pattern on both faces as shown in Figure 3 [11].

Taft earthquake was chosen for the out-of-plane target ground motion. The acceleration response spectrum of this motion when scaled to 0.4g compared well with the design response spectrum specified in the Indian seismic code IS 1893 for PGA=0.36g as shown in Figure 4a [15]. The Taft motion with 0.4g peak acceleration is referred as Level V motion and when scaled to 0.05, 0.11, 0.18, and 0.27g are denoted as Levels I, II, III, and IV motions, respectively. The in-plane loading consists of displacement-controlled slow cycle of gradually increased story drifts from 0.10% to 2.20% as per ACI 374.1 [16].

The developed test procedure and loading sequence are summarized in Figure 4b. The test started with the out-of-plane shake table motions consisting of a series of Taft motions from Levels I to V. After the completion of this out-of-plane loading schedule, the wall was subjected to quasi-static in-plane cyclic loading and continued until cracks were visible (till 0.50% drift cycle). Subsequently,

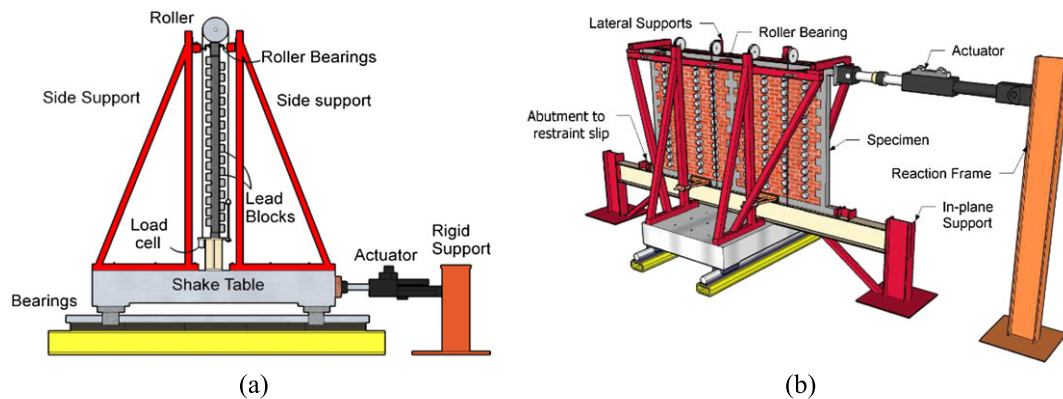


Figure 3. Schematic showing various components of the test setup: (a) out-of-plane loading and (b) in-plane loading.

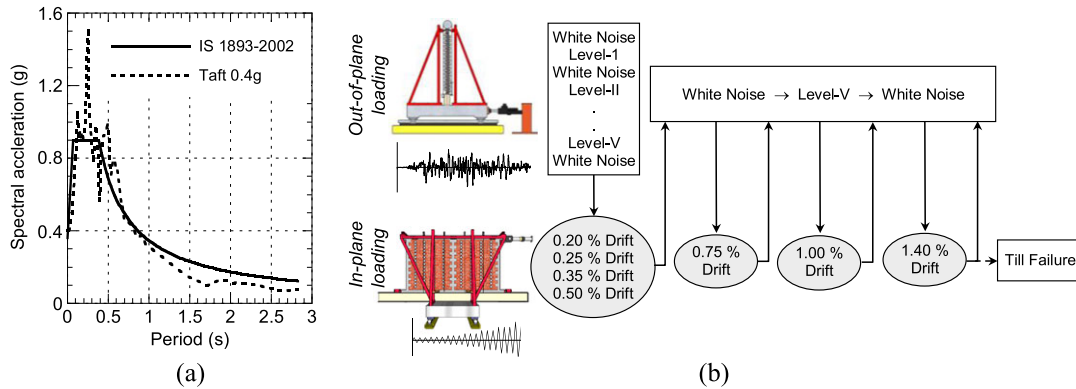


Figure 4. (a) Comparison of scaled response spectra of DBE (design basis earthquake) and original Taft motion upscaled to 0.4g. (b) Summary of test procedure and loading sequence.

the out-of-plane loading was applied, which consists of only Level V Taft motion, and an alternate process of in-plane and out-of-plane loading was continued until the specimen failed [2]. This loading program addresses the issue of reduction in the out-of-plane resistance of a wall because of prior in-plane damage under a realistic out-of-plane shake table motions corresponding to a given hazard level. The cyclic in-plane drift cycles (damage levels) can be thought to correspond various target drifts assumed in a displacement based design method.

2.3. Results and discussion

The failure patterns of all specimens at the end of the test along with key observations and hysteretic behavior are illustrated in Figures 1 and 2. The infill masonry walls showed separation of masonry panel with confining frame even at low in-plane drift level of 0.2%. However, CM walls did not experience any such separation till the drift cycle of 1.75%. The CM construction strengthened the wall to tie-column interaction and helped reduce the likelihood of out-of-plane instability. These CM walls behaved more like a shear wall with RC tie-columns as boundary elements. No appreciable difference in overall behavior was noted in walls SC_{CT} and SC_{FT}, suggesting that both types of tothing were nearly equally effective. However, specimen SC_{FT} with higher density of tothing, demonstrated a more uniform distribution of cracks.

The wall with only lintel beam (SI-O_{2WA}) developed large cracks at the edges of opening, experienced considerable distortion across the openings, and the masonry around openings became highly vulnerable to out-of-plane dislodgement. Walls SC-O_{2WB} and SC-O_{DWB} with no continuous horizontal band suffered severe damage to masonry piers at higher drift levels (>1.4% drift), which imply inadequate confinement to piers in these walls. However, the wall with continuous horizontal band (SC-O_{2WC}) below and above the opening demonstrated uniform distribution of cracks over the entire wall panel, and no major cracks were observed in piers, spandrels, and confining elements even after 2.2% in-plane drift cycle.

The observed in-plane response in terms of ultimate load, hysteretic energy dissipated, and strength degradation (ratio of residual strength and peak load) are listed in Table I. Residual strength is taken as load carried by the wall at the end of test or at last in-plane drift/displacement cycle before failure. The envelope curves for all walls are compared in Figure 5. The wall SC_{FT} with high density of tothing and wall SC-O_{2WC} with continuous horizontal bands maintained the in-plane resistance with less than 20% strength degradation even after the 1.75% drift cycle. As observed from Table I and Figure 5, both CM walls SC_{FT} and SC-O_{2WC} performed better than other walls because of higher in-plane capacity and reduced rate of strength and stiffness degradation in the post-peak range. Confining an opening on all four sides clearly improved both in-plane and out-of-plane response, and wall panels were able to compensate for deficiencies in strength/stiffness/energy dissipation capacity because of openings. The in-plane capacities of walls SC-O_{2WB} and SC-O_{2WC} were found to be about 44% and 80% higher than the perforated infill wall SI-O_{2WA}, respectively. The scheme

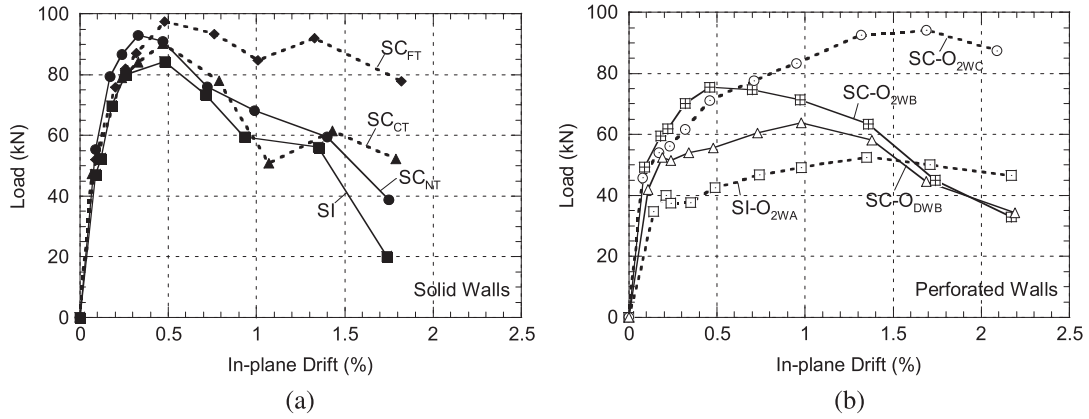


Figure 5. Comparison of observed envelope value of load versus story drift: (a) solid walls and (b) walls with openings.

C with continuous sill and lintel bands was also able to ‘recover’ loss in strength because of the presence of openings.

The peak out-of-plane displacements of masonry panels in solid walls and masonry piers A, B, and C in perforated walls after each in-plane drift (damage) level are compared in Figure 6. The solid wall SI with infilled masonry showed continuous increase in out-of-plane deflection with the in-plane damage and was likely to collapse after 1.75% drift cycle (Figure 6a). In contrast, the maximum out-of-plane displacements in solid CM walls (SC_{CT} , SC_{FT} , and SC_{NT}) remain fairly invariable with the in-plane damage as shown in Figure 6a. For perforated walls $SI-O_{2WA}$ and $SC-O_{2WC}$, the mean of peak out-of-plane displacement recorded in piers B_1 and B_2 were compared with pier B of other walls as shown in Figure 6b–6d. Due to the severe damage to masonry piers in walls $SI-O_{2WA}$, $SC-O_{2WB}$, and $SC-O_{DWB}$, significant out-of-plane displacements were observed in these walls when compared with the wall $SC-O_{2WC}$ (Figure 6b–6d). As depicted from Figure 6d, the central pier B in the wall $SC-O_{DWB}$ experienced large out-of-plane deformation and was on the verge of collapse. In contrast, the peak out-of-plane displacement in the wall $SC-O_{2WC}$ with continuous lintel and sill band remains fairly invariable with the in-plane damage (Figure 6b–6d). The bidirectional response of CM walls demonstrated that their out-of-plane response was not significantly affected by the prior in-plane damage; this is primarily attributed to the composite action developed between the wall and tie-columns.

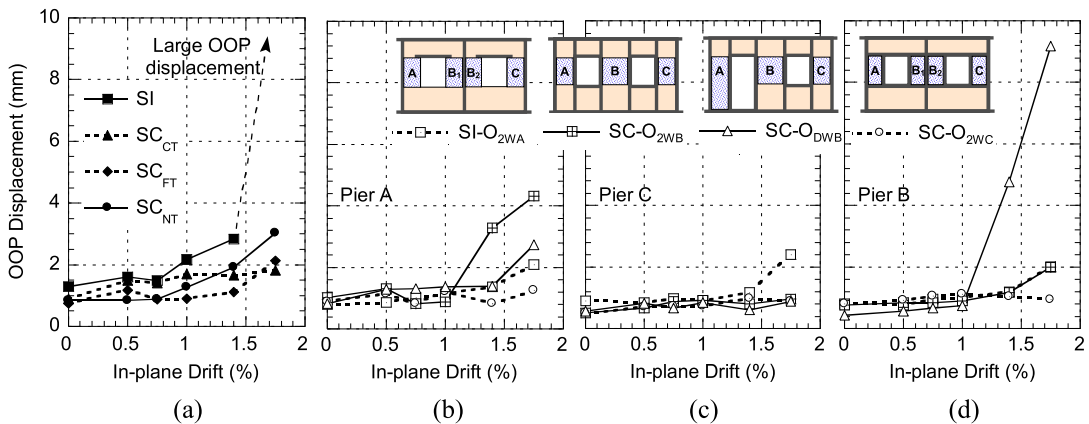


Figure 6. Variation in out-of-plane displacement with in-plane drift/damage: (a) solid masonry walls, (b)–(d) walls with opening in pier A, C, and B. OOP, out-of-plane.

3. IN-PLANE STRENGTH AND STIFFNESS PREDICTION OF CONFINED MASONRY WALLS

3.1. In-plane shear strength

Under seismic loads, shear failure is the most common type of failure of a CM wall because of its typical material behavior and the geometry of structural walls [17]. For estimating the shear resistance of CM walls, two different theories have been developed to physically model the shear failure mechanism of masonry. In the first hypothesis, the shear strength of CM wall is derived based on the friction theory as given by Equation (1).

$$R_{w,s} = (Xv_{mo} + Y\sigma_o)A_w \quad (1)$$

where v_{mo} is the shear strength under zero compression stress, σ_o is the design compressive stress, and A_w is the cross-sectional area of the wall. The X and Y are constants defining the contribution of v_{mo} and σ_o , respectively. The value of constants X and Y in Equation (1) has been proposed by many researchers based on the regression analysis of experimental results. For CM walls, the proposed values of constants X and Y typically varies from 0.21–0.60 and 0.23–0.37, respectively (Table II). A significantly larger range of constant X can be attributed to great disparity in materials used and construction techniques in past experimental studies. To provide a practical and straightforward method for the design of CM walls according to the friction theory, many international standards and earlier research studies neglect the contribution of longitudinal reinforcement in tie-columns. The aim of various in-plane shear models provided by international codes and researchers was to capture the strength at first cracking [18, 19, 21, 22]. However, it is not explicitly stated that the estimated strength will be at first cracking or at failure of the CM wall.

The second approach to evaluate the shear resistance of masonry is based on the assumption of elementary theory of elasticity [32]. According to this hypothesis, when the wall is subjected to both vertical and lateral loads, the shear failure due to the formation of diagonal cracks are caused by principal tensile stresses, which develop in plane of the wall. Thus, by considering masonry as an elastic, homogenous, and isotropic structural element, the lateral resistance, $R_{w,s}$, of plain masonry wall failing in shear can be derived as given by the following equation [12]:

$$R_{w,s} = A_m \frac{f_m^t}{\beta_s} \sqrt{\frac{\sigma_o}{f_m^t} + 1} \quad \text{with} \quad \beta_s = \min\left(\frac{H_w}{L_w}, 1.5\right) \geq 1.0 \quad (2)$$

where f_m^t is the tensile strength of the masonry, and β_s is the shear stress distribution factor, which primarily depends on the height H_w and length L_w of the wall. In case of CM walls, the part of shear capacity of the wall can also be attributed to the tie-column reinforcement. The vertical reinforcement in tie-columns contributes to shear capacity because of the dowel action [29]. Therefore, the maximum lateral resistance, R_{max} of the CM wall can be obtained by adding the shear resistance provided by the brick panel $R_{w,s}$ and vertical rebars, $R_{rv,d}$ (Equation (3)). Different approaches have been adopted in earlier research studies to evaluate the shear resistance provided by the longitudinal reinforcement.

$$R_{max} = R_{w,s} + R_{rv,d} \quad (3)$$

The existing relations for predicting the lateral resistance of CM walls are presented in Table II; the in-plane strength is designated as R_{max-AB} where alphabets AB signify the initials of authors involved in developing a particular relation/model. The first 10 models presented in Table II (Equations 4 to 13) were established assuming a friction theory, that is, first hypothesis (will be further denoted as HT1). The models proposed in the Argentinean code [18], Colombian code [21], and by Moroni *et al.* [20] are almost identical and consist of two variables, v_{mo} and σ_o . The strength prediction equations given by D'Amore and Decanini [19] and San Bartolomé *et al.* [22] were also based on first hypothesis and introduced a correction factor to account for aspect ratio of the wall.

Among first 10 models in Table II, four equations (Equations 10 to 13) include the contribution of longitudinal reinforcement in the shear capacity of confined walls. Marinilli and Castilla [13] based on their experimental results and regression analysis simply accounted for longitudinal reinforcement

Table II. Existing models for maximum shear strength of confined masonry walls.

ID	Equation	Remark	Reference
R_{max-AC}	$(0.6v_{mo} + 0.3\sigma_o)A_w$ (4)	—	Inpres Cirsoc [18]
R_{max-DD}	$(0.6v_{mo} + 0.3\sigma_o)k_f A_w$ (5)	$k_t = \min\left(1.2 - \frac{0.2H_w}{L_w}, 1\right)$	D'Amore and Decanini [19]
R_{max-MO}	$\min(0.45v_{mo} + 0.3\sigma_o, 1.5v_{mo})A_w$ (6)	—	Moroni <i>et al.</i> [20]
R_{max-CO}	$\min\left[\left(\frac{\sqrt{f_m^{c'}}}{12} + \frac{\sigma_o}{3}\right)A_w, \frac{\sqrt{f_m^{c'}}}{6}A_w\right]$ (7)	—	Colombia code [21]
R_{max-BA}	$(0.5v_{mo}\alpha + 0.23\sigma_o)A_w$ (8)	$1/3 \leq \alpha (= V_e L_w / M_e) \leq 1$	San Bartolome <i>et al.</i> [22]
R_{max-ML}	$\left[1.0072 + 0.4897v_{mo} + 0.5341\sigma_o - 0.137\left(\frac{H_w}{L_w}\right) - 0.9966\left(\frac{A_m}{A_w}\right)\right]A_w$ (9)	A_m/A_w is the masonry panel cross-section area given by the relation between masonry panel area and total wall area	Marques and Lourenço [23]
R_{max-MA}	$\left[k_u k_p \left(\frac{0.76}{\frac{H_w}{d} + 0.7} + 0.012\right) \sqrt{f_m^{c'}} + 0.2\sigma_o\right] t_w j$ (10)	$k_u = 1.0$ for solid masonry walls $j = 7/8d, d = L_w - w_{ic}/2$ $k_p = 1.16\rho_{icm}^{0.3}, \rho_{icm} = A_s N_{ic} / t_w L_w$	Matsumura [24]
R_{max-FA}	$(0.5v_{mo} + 0.3\sigma_o)A_w + \eta_F \left(1.26md_f^2 \sqrt{f_c f_y}\right)$ (11)	$\eta_F = 0.3$	Flores and Alcocer [25]
R_{max-MC}	$(0.47v_{mo} + 0.29\sigma_o)(A_w - N_{ic}A_{ic}) + 4200N_{ic}$ (12)	Units are in kg/cm	Marinilli and Castilla [13]
R_{max-RI}	$\left(0.21v_{mo} + 0.363\sigma_o + 0.0141\sqrt{\rho_{ic} f_y^{c'}}\right)A_w$ (13)	—	Riahi <i>et al.</i> [26]

1st hypothesis: Friction theory (HT1)

(Continues)

Table II. Continued

ID	Equation	Remark	Reference
R_{max-TK}	$\frac{f'_m A_w}{C_i \beta_s} \left[1 + \sqrt{C_i^2 \left(1 + \frac{\sigma_o}{f'_m} \right) + 1} \right] + \sum_{i=1}^n 0.806 d_i^2 \sqrt{f'_c f_y} \quad (14)$	$C_i = 2\alpha_i \beta_s \frac{L_w}{h_w}$ $\alpha_i = 5/4 =$ parameter for distribution of interaction force	Tomažević and Klemenc [12, 27]
R_{max-LA}	$f'_m \frac{a_w}{L_w} \left(\frac{H_w}{L_w} + \sqrt{\frac{H_w}{L_w} + 4 + \frac{4\sigma_o}{f'_m}} \right) A_w \quad (15)$	$a_w/L_w = 0.56, 0.65$ and 0.85 for $H_w/L_w = 1.21, 1.01$ and 0.76 $R_{v,d} =$ max. value of shear resistance due to dowel action of single bar $= \max \left(\frac{2}{3} R_{cb}, \frac{1}{3} R_{cb} + R_{st} \right)$	Lafuente <i>et al.</i> [28]
R_{max-BO}	<p>Failure by critical tensile stress:</p> $A_w \frac{f'_m}{\beta_s} \sqrt{\frac{\sigma_o}{f'_m} + 1} + \sum_{i=1}^n R_{rv,d(i)} \quad (16a)$	$R_{cb} =$ reaction of the concrete on the main bar and is estimated by solving following quadratic equation $\frac{0.256}{f'_c d_l} R_{cb}^2 + \frac{2f_{y,ast}}{f'_c d_l} R_{cb} - \frac{16f_{y,ast}^3}{32} = 0$	Bourzam <i>et al.</i> [29]
	<p>Failure by biaxial combination of principal stresses:</p> $\frac{A_w/\beta_s}{\left(1 + \frac{f'_m}{f'_m} \right)} \sqrt{f_m'^2 + \sigma_o f'_m \left(1 - \frac{f'_m}{f'_m} \right) - \sigma_o^2 \frac{f'_m}{f'_m} + \sum_{i=1}^n R_{rv,d(i)}} \quad (16b)$	$R_{st} = f_{y,ast} =$ reaction of stirrup on the main bar $\eta_c =$ confinement factor for wall $= 1.0$ for tie-column spacing > 2.8 m $= 1.1$ for tie-column spacing < 2.8 m $\zeta_n =$ participating factor of intermediate tie-columns $= 0.5$ for only one tie-column and 0.4 for other cases $v_{em} = \frac{v_{mo}}{1.2} \sqrt{1 + \frac{\sigma_o}{v_{mo}}} \quad (17)$	Chinese code [30]
R_{max-CH}	$\left[\eta_c v_{em} (A_w - A_{cn}) + \zeta_n f'_c A_{cn} + 0.08 f_y A_{st} \right] \quad (17)$		
R_{max-RA}	$R_{nc} \left(2.15 + 0.7 \left(\frac{l_{i,t}}{p} \right) \right) \quad (18)$	$R_{nc} =$ strength of masonry wall with no confinement $l_{i,t} =$ total centerline length of internal confining elements $p =$ centerline length of confining elements at the perimeter	Rai <i>et al.</i> [31]

All dimensions are in N and millimeters (mm) except were mentioned.

through number of tie-columns N_{tc} present in a CM wall (Equation (12)). The model developed by Matsumura [24] and Riahi *et al.* [26] do consider the contribution of tie-columns through total longitudinal reinforcement ratio ρ_{lc} (Equations (10) and (13)) but did not account for the number of tie-columns present in the CM wall. This approach will be more appropriate when the reinforcement is uniformly distributed over the entire length of the wall such as in case of reinforced masonry construction. Marques and Lourenço [23] used advanced statistical and nonlinear regression analyses on a database of 105 tested walls to derive the predictive model for the shear capacity of CM walls. Based on the sensitivity analysis, Marques and Lourenço [23] concluded that longitudinal reinforcement of tie-columns has an insignificant influence on the shear strength of CM walls. However, this observation is in contrast to other strength relations that recognize the contribution of tie-column reinforcement on its shear capacity.

The model proposed by Tomažević and Klemenc [12, 27] is based on the stress condition at the center of wall (second hypothesis, HT2) and also considers the shear resistance because of the interaction forces C_i , which develops at the interface between confining elements and masonry panel when subjected to lateral loading. Bourzam *et al.* [29] further extended the methodology of Tomažević and Klemenc [12, 27] and also proposed a model to evaluate maximum shear resistance of wall when the failure is governed by the biaxial combination of principal stresses (Equation (16b)). The shear capacity of the CM wall as per Bourzam *et al.* will be the minimum value obtained from two failure criteria (Equations (16a) and (16b)). Both models considered the lateral strength contribution from the dowel action of the longitudinal rebars in tie-columns. Lafuente *et al.* [28] also proposed an expression based on the theory of elasticity and calibrated it to approximate the experimental results but neglected the contribution of longitudinal reinforcement.

The predictive relationships proposed by the Chinese code [30] and Rai *et al.* [31] are categorized as third hypothesis (HT3). The Equation (17) proposed in the Chinese code [30] defines a new variable, v_{em} , which represents the shear strength along the stair-stepped damage of the masonry. This relationship only takes into account the contribution of tie-columns installed in the middle of the wall. Rai *et al.* [31] proposed a simple method to estimate the performance parameters of walls sub-paneled with RC elements. These sub-paneled walls consist of load bearing infill masonry confined by a framework of connected RC elements. Based on the experimental and numerical analyses, strength and stiffness of the sub-paneled walls were directly correlated with the degree of confinement (Equation (18)) [31]. The degree of confinement provided in a wall was specified by a confinement factor defined as the ratio of the total centerline length of internal confining elements (tie-beams and tie-columns), $l_{i,t}$ to the centerline length of confining elements at perimeter of the wall, p . In the proposed Equation (18), the in-plane shear strength R_{nc} of unconfined masonry walls was estimated using the Equation (19) [33].

$$R_{nc} = \min \left\{ \begin{array}{l} A_w(0.2 + 0.4\sigma_o) \\ 0.25\sqrt{f_m^c} \end{array} \right. \quad (19)$$

The role of intermediate confining elements is not recognized by the majority of available relationships. Experimental study conducted by Marinilli and Castilla [13] and Rai *et al.* [31] showed that the inclusion of the interior tie-columns can significantly enhance the ductility, peak capacity, and damage distribution of masonry walls. However, the relationship proposed by Chinese code [30] and Rai *et al.* [31] only explicitly considered the contribution of intermediate tie-column in CM walls. On the contrary, most of the models did not differentiate between interior and boundary confining elements and simply considered total amount of reinforcing steel provided in CM walls [13, 24–27, 29].

3.2. In-plane stiffness

The elastic stiffness K_{el} of a masonry wall can be defined by taking into consideration for the shear and flexural deformation of the wall under lateral loads. Using similar approach, Flores and Alcocer [25], Tomažević and Klemenc [12], and Bourzam *et al.* [29] derived the elastic stiffness of the CM wall. Various existing models to predict the in-plane stiffness of CM walls are listed in Table III. Tomažević and Klemenc [12] defined cracked or secant stiffness of the wall as a function of elastic stiffness and extent of damage in walls (damage index I_d). As shown in Equation (21), two stiffness

Table III. Existing models for the in-plane stiffness of confined masonry walls.

ID	Equation	Remark	Reference
K_{el}	$\frac{G_{eqv}A_w}{kH_w \left[1 + \alpha' \frac{G_{eqv}}{E_{eqv}} \left(\frac{H_w}{L_w} \right)^2 \right]} \quad (20)$	$E_{eqv} = \frac{E_m A_m + \sum E_c A_{ci}}{A_m + \sum A_{ci}}$ $G_{eqv} = \frac{G_m A_m + \sum G_c A_{ci}}{A_m + \sum A_{ci}}$ <p>$\alpha' = 0.33$ for cantilever wall and 0.83 in case for the fixed-ended wall $k = 1.2$ = the shear coefficient for rectangular cross-section</p>	Tomažević and Klemenc [12] and Bourzam <i>et al.</i> [29]
K_{cr-TK} $K_{Rmax-TK}$	$K_{el} - \sqrt{aI_d - b} \quad (21)$	I_d = damage index a and b are the stiffness degradation parameters	Tomažević and Klemenc [12]
K_{cr-RI}	$A_w \frac{\sqrt{f_m^c}}{\gamma_c H_w} \quad (22)$	$\gamma_c = \begin{pmatrix} 1.13, & \text{for clay brick} \\ 0.72, & \text{for concrete block} \end{pmatrix}$	Riahi <i>et al.</i> [26]
K_{cr-RA}	$K_{nc} \left(0.29 + 0.26 \left(\frac{l_{i,t}}{p} \right) \right) \quad (23)$	$K_{nc} = \left[\left(\frac{H_w^3}{3E_m I_m} \right) + \left(\frac{H_w}{A_w G_m} \right) \right]^{-1}$	Rai <i>et al.</i> [31]
$K_{Rmax-RI}$	$A_w \frac{\sqrt{f_m^c}}{0.65 \mu \gamma_c H_w} \quad (24)$	$\mu = \left[0.5 \left(\frac{A_w}{R_{max}} \right)^2 + 1.3 \right] \leq 6$ $R_{max} = \text{same as } R_{max-RI}$	Riahi <i>et al.</i> [26]

degradation parameters a and b were proposed. Based on the boundary conditions and experimental results, Tomažević and Klemenc [12] obtained the value of these parameters a and b as $1.281 K_{el}^2$ and $0.320 K_{el}^2$, respectively.

Using the Equation (21) in Table III and damage indices I_d , the stiffness of CM wall can be estimated at various damage levels. In the present study, the measured stiffness K_{cr} and K_{Rmax} at the cracking load R_{cr} and peak load R_{max} , respectively, were compared with the values predicted using the existing models. The stiffness K_{cr} is same as effective stiffness K_e mentioned earlier. Bourzam *et al.* [29] used the identical approach to derive the secant stiffness of CM walls but proposed the different values of degradation parameters a and b as $1.805 K_{el}^2$ and $0.451 K_{el}^2$, respectively. Rai *et al.* [31] correlated the stiffness at initial cracking with the confinement factor $l_{i,t} / p$ as given by Equation (23), which also considered the role of interior tie-columns. The stiffness of CM walls at the cracking and peak load was also estimated through the backbone model proposed by Riahi *et al.* [26], and these derived equations are listed in Table III.

3.3. Comparison of predicted strength and stiffness with test results of solid confined masonry walls

The lateral load capacity of CM walls SC_{CT}, SC_{FT}, and SC_{NT} obtained from tests are compared with values predicted using the existing relations. The shear strength under zero compression v_{mo} and the tensile strength of masonry f_m^t was calculated using the following equations [34, 35].

$$v_{mo} = 0.184 \sqrt{f_m^c} \quad (25)$$

$$f_m^t = 0.125 \sqrt{f_j^c} \text{ where, } f_j^c \text{ is the compressive strength of joint mortar} \quad (26)$$

The shear strength v_{mo} and tensile strength f_m^t of masonry estimated from Equations (25) and (26) are in range of 0.50 to 0.59 MPa and 0.29 to 0.34 MPa, respectively. These values correlate well with

the initial shear and tensile strength values obtained from the series of tests performed by Singhal and Rai [14] on masonry with similar lime-cement mortar mix.

The ratio R_{exp}/R_{cal} obtained from all 15 existing models is plotted in Figure 7, and for a reasonable prediction of strength, this ratio should be nearly equal to 1.0. Existing models based on the first hypothesis that neglect the contribution of the longitudinal reinforcement (Equations 4 to 9), highly underestimated the shear capacity of CM walls. This is indicated by significantly higher values of ratio R_{exp}/R_{cal} (>1.75) in Figure 7. Also, many models aim to capture the strength at first cracking, thereby providing conservative estimates of the shear strength of CM walls (Equations (4), (5), (7), and (8)). However, by considering the contribution of longitudinal reinforcement in tie-columns (Equations 10 to 13), the first hypothesis provided relatively better estimate of shear capacity of CM walls except for the Equation (10) proposed by Matsumura [24]. This equation predicted significantly higher value of in-plane strength as the ratio R_{exp}/R_{cal} was obtained nearly equal to 0.55.

The existing relations based on second hypothesis from Equations (14) to (16) slightly overestimate the observed values and provided prediction within an error of approximately 25% (Figure 7). The most accurate prediction of shear capacity (with a maximum error of 7%) was made by the strength relation proposed in the Chinese code [30]. The accurate prediction by this relation indicates that the contribution of longitudinal reinforcement in interior tie-columns is important; however, the role of reinforcement in tie-columns located at the perimeter of wall can be ignored. The simple method

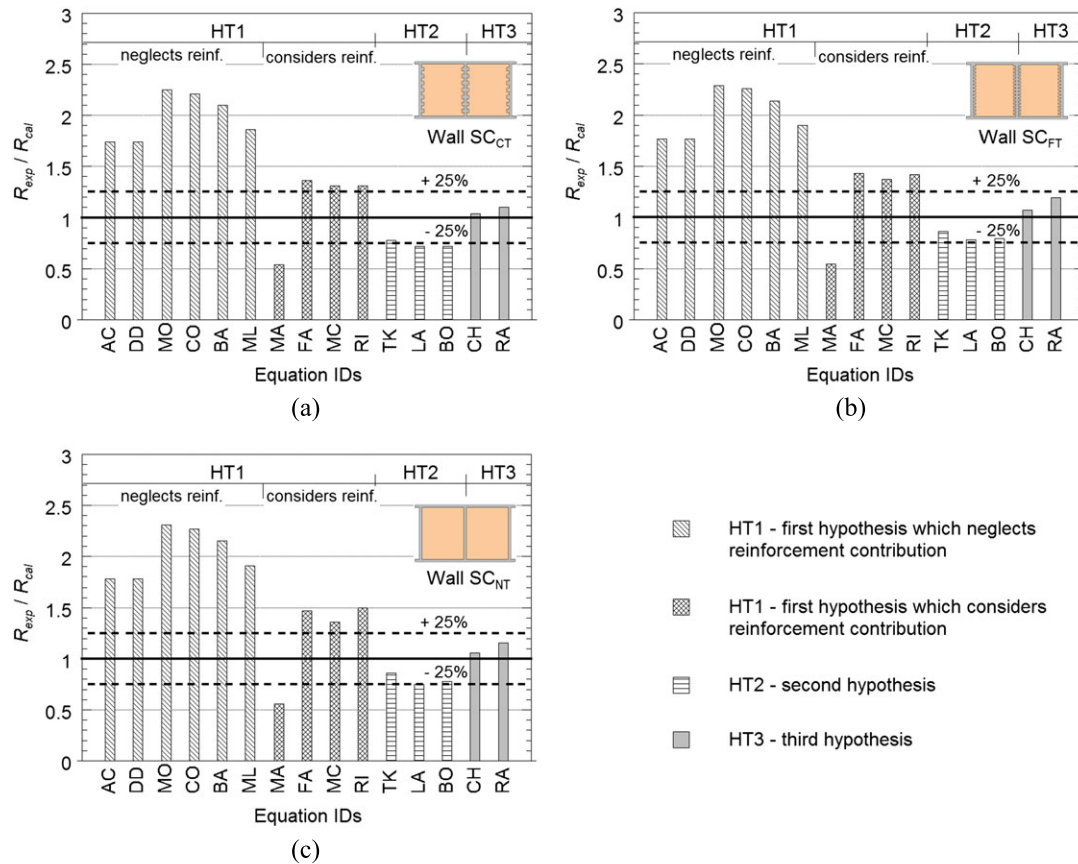


Figure 7. Comparing accuracy of existing model to predict the shear resistance of solid confined masonry walls: (a) SC_{CT} , (b) SC_{FT} , and (c) SC_{NT} . Note that the alphabetical notations (IDs) refer to equations proposed by particular researchers or in a national standards: AC, Argentinean Code [18]; DD, D'Amore and Decanini [19]; MO, Moroni *et al.* [20]; CO, Colombia Code [21]; BA, San Bartolome *et al.* [22]; ML, Marques and Lourenço [23]; MA, Matsumura [24]; FA, Flores and Alcocer [25]; MC, Marinilli and Castilla [13]; RI, Riahi *et al.* [26]; TK, Tomažević and Klemenc [12]; LA, Lafuente *et al.* [28]; BO, Bourzam *et al.* [29]; CH, Chinese Code [30]; and and RA = Rai *et al.* [31].

proposed by Rai *et al.* [31], which is based on the simple measure of degree of confinement, provides reasonable estimate for the lateral strength of CM walls.

The predicted values of stiffness K_{cal} for each wall at the cracking load R_{cr} and peak load R_{max} are compared with experimental values in Figure 8. This comparison clearly indicates that only the method proposed by Rai *et al.* [31] closely predicts the cracking stiffness of all solid wall specimens. The equations given by Tomažević and Klemenc [12] and Bourzam *et al.* [29] significantly overestimated both stiffness values K_{cr} and K_{Rmax} , and therefore, the proposed stiffness degradation parameters a and b need to be adjusted and revised. Riahi *et al.* [26] provided a reasonable prediction of stiffness values within 25% for wall specimens SC_{CT} and SC_{FT}; however, for wall SC_{NT}, the predicted values were noticeably lower than the measured stiffness. It should be noted that the available formulas should also be validated for walls with different aspect ratio (H/L ratio). In this study, the specimens had aspect ratio (H/L) of 0.6 when considering the full length of the wall (2.5 m) whereas H/L ratio is 1.23 when the distance between two tie-columns (1.22 m) is considered.

4. REDUCTION FACTOR FOR CONFINED MASONRY WALLS WITH OPENINGS

The effects of openings on the strength and stiffness of masonry walls were usually taken into consideration in many previous research studies through reduction factors D_F . The reduction factor is generally defined as the ratio of strength or stiffness of a perforated masonry to that of an identical solid masonry. Due to the lack of research on CM walls with openings [3, 36], these reduction factors were primarily proposed for masonry infilled frames. For CM walls with openings, Riahi *et al.* [26] was first to propose a reduction factor for the cracking shear strength R_{cr} . Moreover, these proposed relations for the reduction factor were based on regression analysis of limited number of test results and thus may be applicable to specific type of wall panels.

In lieu of scarcity of detailed analytical study on CM walls with openings, the suitability of various reduction factors originally developed for masonry infilled frame will be reviewed in this section. Mohammadi and Nikfar [37] provided a summary of various empirical relations of reduction factors available in the literature and also proposed a new reduction factor for strength and stiffness of masonry infilled frames having central openings. The existing equations of reduction factors for strength, DR_F , and stiffness, DK_F , of perforated masonry walls are summarized in Table IV. As can be seen in Table IV, Al-Chaar *et al.* [38] and New Zealand Society of Earthquake Engineering (NZSEE) [39] proposed a common equation for both strength and stiffness reduction, whereas Mohammadi and Nikfar [37] developed separate empirical equations for DR_F and DK_F . Moreover, equations proposed by Riahi *et al.* [26] and Tasnimi and Mohebkah [41] were only derived for the reduction in strength of the wall, while Mondal and Jain [40] and Asteris *et al.* [42] formulated the reduction factors for initial stiffness of the infill wall.

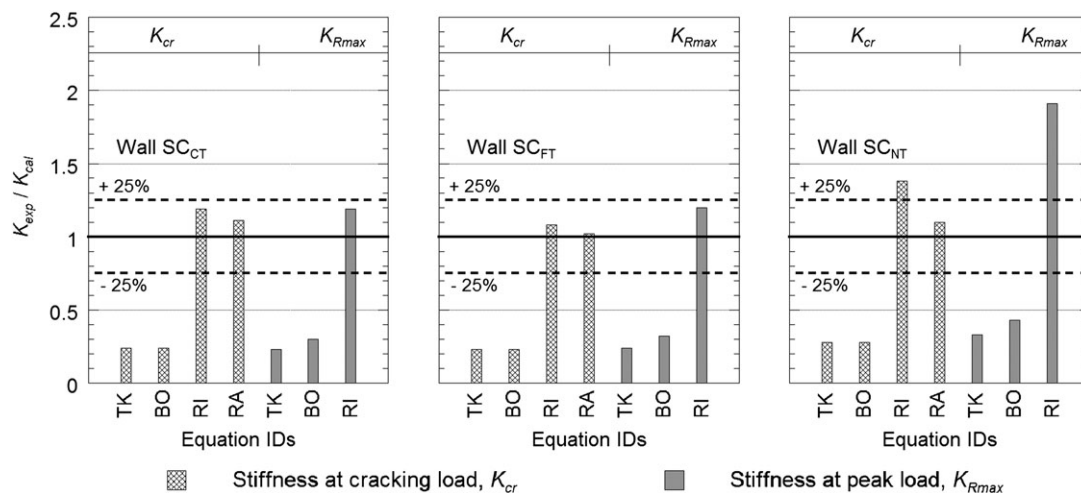


Figure 8. Comparing accuracy of existing model to predict the stiffness of solid confined masonry walls.

Table IV. Strength and stiffness reduction factor to account for the presence of opening.

ID	Equation	Remark	Reference
DR_{F-AL}	$0.6(A_r)^2 - 1.6(A_r) + 1$ (27)	$A_r =$ ratio of area of the opening and wall panel $= A_o/A_p$	Al-Chaar <i>et al.</i> [38]
DK_{F-AL}	same as previously		
DR_{F-NZ}	$1 - 1.5 \frac{l_o}{l_w}$ (28)	—	NZSEE [39]
DK_{F-NZ}	same as previously		
DR_{F-MJ}	—	Valid only for window openings located at the center of masonry panel	Mondal and Jain [40]
DK_{F-MJ}	$1 - 2.6(A_r)$ (29)		
DR_{F-RI}	$-2.2(A_r) + 1$ (30)	—	Riahi <i>et al.</i> [26]
DK_{F-RI}	—		
DR_{F-TM}	$1.49(A_r)^2 - 2.238(A_r) + 1$ (31)	For $\frac{A_o}{A_w} > 0.4$, $DR_{F-TM} = 0$	Tasnimi and Mohebbkhah [41]
DK_{F-TM}	—		
DR_{F-AS}	—		Asteris <i>et al.</i> [42]
DK_{F-AS}	$1 - 2(A_r)^{0.54} + (A_r)^{1.14}$ (32)		
DR_{F-MF}	$-1.085(A_r) + 1$ (33)	Valid for $\frac{A_o}{A_w} \leq 0.4$	Mohammadi and Nikfar [37]
DK_{F-MF}	$1.186(A_r)^2 - 1.678(A_r) + 1$ (34)		

As shown in Table IV, the proposed reduction factors are generally the function of the area ratio of opening and wall panel ($A_r = A_o/A_p$) except for the factor given by NZSEE [39]. The reduction factor prescribed by NZSEE is given by Equation (28), where l_o and l_w are maximum width of the opening and masonry wall, measured across a horizontal plane, respectively. In contrast to other models, this equation determines the reduction factor based on the opening width and does not account for the effect of height of the opening. This implies that door and window openings of similar width will experience same reduction in the strength and stiffness. However, many research studies had concluded that the wall with door opening exhibited larger reduction in strength and stiffness properties as compared with the window opening of similar width; thus, the equation given by NZSEE should be used with caution.

4.1. Comparison of predicted strength and stiffness with test results of perforated confined masonry walls

The accuracy and reliability of the existing relations of reduction factors was judged by first comparing the predicted values with the ratio of strength and stiffness of a perforated infill wall SI-O_{2WA} to that of the similar solid wall SI. The peak load carrying capacity of walls SI and SI-O_{2WA} was found to be 84.2 and 52.4 kN while, the observed initial stiffness values were 32.4 and 17.1 kN/mm, respectively. The ratio $A_r (=A_o/A_p)$ for the wall SI-O_{2WA} with two window openings is 0.191. The experimental and predicted values of strength and stiffness reduction factors are compared for infilled wall SI-O_{2WA} in Table V. The equation given by Tasnimi and Mohebbkhah [41] and Mondal and Jain [40] accurately predicts the observed reduction in strength and stiffness of the infilled frame, respectively. Equations (28), (33) and (34) given by NZSEE [39] and Mohammadi and Nikfar [37] showed maximum error in predicting both strength and stiffness reduction for the infill wall. The reduction factor proposed by

Table V. Comparison between the experimental and predicted values of reduction factor for masonry infilled frame with window openings.

Factor	Exp.	AL	NZ	MJ	RI	TM	AS	MN
DR_F	0.62	0.72	0.37	—	0.58	0.63	—	0.79
Error (%)		16	40	—	06	02		27
DK_F	0.53	0.72	0.37	0.50	—	—	0.33	0.72
Error (%)		36	30	06	—	—	38	36

The alphabetical notations AL, NZ, MJ, RI, TM, AS, and MN signify the initials of authors who proposed a particular reduction factor: AL, Al-Chaar *et al.* [38]; NZ, New Zealand Code [39]; MJ, Mondal and Jain [40]; RI, Riahi *et al.* [26]; TM, Tasnimi and Mohebbkhan [41]; AS, Asteris *et al.* [42]; and MN = Mohammadi and Nikfar [37].

Al-Chaar *et al.* provides reasonable predictions and will be further used to estimate the in-plane strength and stiffness of CM walls with openings because of its simple and common relationship for both strength and stiffness. Mohammadi and Nikfar [37] also reported that the equation proposed by Al-Chaar *et al.* [38] estimates both initial stiffness and ultimate strength of the masonry walls with window and door openings more accurately than the other existing empirical formulas.

The shear capacity and cracked stiffness of perforated CM walls obtained from the test are compared with predicted values by calculating the ratio R_{exp}/R_{cal} , K_{exp}/K_{cal} as presented in Figure 9. The in-plane strength and stiffness was calculated by first considering the perforated wall as a solid wall and then estimating the strength and stiffness by applying the reduction factors DR_F and DK_F proposed by Al-Chaar *et al.* as discussed previously. For strength estimation, only those equations were chosen, which include the contribution of the confining columns in the wall. However, all the available methods were used for estimating the stiffness K_{cr} at the cracking load (Equations 21 to 23).

As illustrated in Figure 9, the simplified method developed by Rai *et al.* [31] predicted both strength and stiffness of all perforated CM walls within an error of 25%. The remaining strength equations only provided good estimate of shear resistance for walls with confining scheme B (CM walls SC-O_{2WB} and SC-O_{DWB} with all vertical confining members extending to full-height of the wall). Moreover except Rai *et al.* [31], the other equations failed to provide reasonable prediction of stiffness at cracking load for CM walls with openings. These existing equations either highly overestimated or underestimated the stiffness K_{cr} of perforated CM walls.

Table VI compares the mean values of ratios $R_{max(exp)}/R_{max(cal)}$ and $K_{cr(exp)}/K_{cr(cal)}$ obtained from the existing and proposed models. Table VI clearly indicates that the simple method developed for sub-paneled walls provide most accurate and reliable predictions for both strength and stiffness of CM walls. However, majority of existing models either greatly overestimate the stiffness [12, 29] or underestimate the shear strength [13, 25] of CM walls and thus may be inappropriate for design purposes (Table VI).

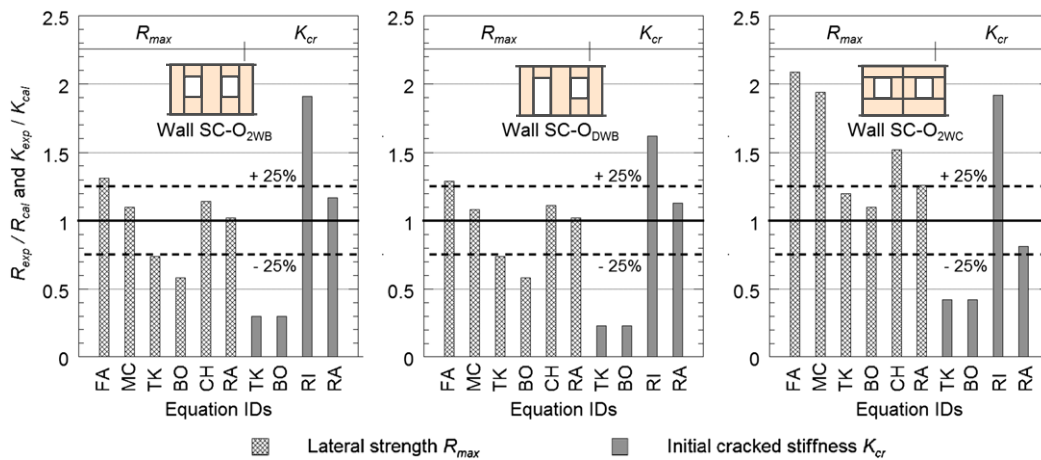


Figure 9. Accuracy of existing model to predict the strength of confined masonry walls with openings.

Table VI. Comparison between the experimental and predicted values of maximum strength and cracked stiffness

Reference ID	$R_{max(exp)}/R_{max(cal)}^*$	$K_{cr(exp)}/K_{cr(cal)}$	Reference
FA	1.49 ± 0.30	—	Flores and Alcocer [25]
MC	1.36 ± 0.31	—	Marinilli and Castilla [13]
RI	—	1.52 ± 0.36	Riahi <i>et al.</i> [26]
TK	0.86 ± 0.17	0.28 ± 0.07	Tomažević and Klemenc [12]
BO	0.76 ± 0.19	0.28 ± 0.07	Bourzam <i>et al.</i> [29]
CH	1.16 ± 0.18	—	Chinese code [30]
RA	1.13 ± 0.10	1.19 ± 0.22	Rai <i>et al.</i> [31]

*Mean \pm standard deviation

5. CONCLUSIONS

An experimental study on CM walls was performed to investigate the role of tothing details at the wall-to-tie-column interface and effect of the presence of openings under bidirectional loading of simulated out-of-plane ground motions and prior damage due to in-plane loading. CM walls maintained structural integrity up to large in-plane drifts of 1.75% and performed much better than masonry infill RC frames. Due to composite action developed between masonry and tie-columns, CM walls acted as structural shear wall for in-plane loads, and their out-of-plane response was not significantly affected by the prior in-plane damage. Tothing at the wall-to-tie-column interface significantly improved the post-peak behavior of CM walls under in-plane loads, and superior performance was observed when tothing was at alternate brick courses. For perforated walls, provision of vertical RC elements along with continuous horizontal bands (sill/lintel bands) around openings proved to be highly beneficial as the wall was able to achieve the in-plane strength close to that of the solid CM wall.

The experimental results were further used for the analytical verification of various existing models to predict the in-plane strength/stiffness of CM walls. The analytical relations for estimating the shear capacity of CM walls are primarily semi-empirical equations, which are based on either friction theory or elementary theory of elasticity. Better shear strength predictions were obtained for those models that included the amount of longitudinal reinforcement in tie-columns. Neglecting the contribution of tie-columns details can highly underestimate the shear capacity of CM walls with low aspect ratio (H/L about 1.0). The existing equations, which considered the shear and flexural deformation of CM walls, failed to reasonably predict their in-plane stiffness.

Strength and stiffness reduction factors originally proposed to incorporate the negative influence of openings in the masonry infill RC frames were used to predict the in-plane strength and stiffness of perforated CM walls. For CM walls with openings, the reduction factor given by Al-Chaar *et al.* [38] was used because of its reasonable predictions and simplicity. The available relations for estimating the strength and stiffness of CM walls could not provide good predictions for such walls with openings. Based on the simple measure of the degree of confinement provided by interior and exterior confining element, the proposed method by Rai *et al.* [31] for sub-paneled masonry walls reliably predicted the in-plane strength and stiffness of CM walls with and without openings. The simplified equations of this method can be very handy for engineers to correctly estimate the design parameters for CM walls. Further, the suitability of available relationships should also be validated for walls with different aspect ratio.

REFERENCES

1. Brzev S. *Earthquake Resistant Confined Masonry Construction*. National Information Centre for Earthquake Engineering. Indian Institute of Technology Kanpur: India, 2008.
2. Singhal V, Rai DC. Role of tothing on in-plane and out-of-plane behavior of confined masonry walls. *Journal of Structural Engineering* 2014; **140**. DOI:10.1061/(ASCE)ST.1943-541X.0000947, 04014053.
3. Yáñez F, Astorza M, Holmberg A, Ogaz O. Behavior of confined masonry shear walls with large openings. *13th World Conference of Earthquake Engineering*, Vancouver, Canada, August 2004; paper no. 3438.
4. Mays GC, Hetherington JG, Rose TA. Resistance-deflection functions for concrete wall panels with openings. *Journal of Structural Engineering* 1998; **124**(5):579–587.
5. Blondet M (Ed). *Construction and Maintenance of Masonry Houses for Masons and Craftsmen* (2nd edn). Pontificia Universidad Católica del Perú: Lima, Peru, 2005.

6. IAEE. *Guidelines for Earthquake Resistant non-Engineered Construction*. revised ed. reprinted by National Information Center of Earthquake Engineering of India, International Association of Earthquake Engineering (IAEE): Tokyo, Japan, 2004.
7. Meli R, Brzev S, Astroza M, Boen T, Crisafulli F, Dai J, Farsi M, Hart T, Mebarki A, Moghadam A. *Seismic Design Guide for Low-rise Confined Masonry Buildings*. Earthquake Engineering Research Institute (EERI): Oakland, CA, USA, 2011.
8. Schacher T. *Confined Masonry for One and Two Storey Buildings in Low-tech Environments – A Guidebook for Technicians and Artisans*. National Information Centre of Earthquake Engineering (NICEE), Indian Institute of Technology Kanpur: Kanpur, India, 2011.
9. Abrams DP, Angel R, Uzarski J. Out-of-plane strength of unreinforced masonry infill panels. *Earthquake Spectra* 1996; **12**(4):825–844.
10. Flanagan RD, Bennett RM. Bidirectional behavior of structural clay tile infilled frames. *Journal of Structural Engineering* 1999; **125**(3):236–244.
11. Komaraneni S, Rai DC, Singhal V. Seismic behavior of framed masonry panels with prior damage when subjected to out-of-plane loading. *Earthquake Spectra* 2011; **27**(4):1077–1103.
12. Tomažević M, Klemenc I. Seismic behavior of confined masonry walls. *Earthquake Engineering and Structural Dynamics* 1997; **26**(10):1059–1071.
13. Marinilli A, Castilla E. Seismic behavior of confined masonry walls with intermediate confining-columns. *8th U.S. National Conference on Earthquake Engineering*, San Francisco, California, USA, 2006; paper no. 607.
14. Singhal V, Rai DC. Suitability of half-scale burnt clay bricks for shake table tests on masonry walls. *Journal of Materials in Civil Engineering* 2014; **26**(4):644–657.
15. Bureau of Indian Standards (BIS). *Indian standard criteria for earthquake resistant design of structure, Part 1: General provisions and buildings. IS 1893, 5th revision*, New Delhi, India, 2002.
16. American Concrete Institute (ACI). *Acceptance criteria for moment frames based on structural testing and commentary, ACI 374.1-05*, ACI Committee 374, Farmington Hills, MI, 2005.
17. Tomažević M. *Earthquake-resistant Design of Masonry Buildings*. Imperial College Press: London, 1999.
18. Inpres-Cirsoc. *Argentinean Code for Earthquake-resistant Constructions, Part III: Masonry Buildings*. INPRES: San Juan, 1983.
19. D'Amore E, Decanini L. Shear strength analysis of confined masonry panels under cyclic loads: comparison between proposed expressions and experimental data. *9th International Seminar on Earthquake Prognostics*, San José, 1994.
20. Moroni MO, Astroza M, Mesias P. Displacement capacity and required story drift in confined masonry buildings. *11th World Conference of Earthquake Engineering*, Acapulco, Mexico, 1996; paper no. 1059.
21. Asociación Colombiana de Ingeniería Sísmica (AIS). *Colombian code for the seismic design and construction, NSR-98*; Bogotá, D. C., Colombia; 1998.
22. San Bartolomé A, Quiñ D, Myorca P. Proposal of a standard for seismic design of confined masonry buildings. *Bulletin of ERS, No. 37*: University of Tokyo, Japan, 2004.
23. Marques R, Lourenço PB. A model for pushover analysis of confined masonry structures: implementation and validation. *Bulletin of Earthquake Engineering* 2013; **11**(6):2133–2150.
24. Matsumura A. Shear strength of reinforced masonry walls. *Proceeding of the 9th World Conference on Earthquake Engineering*, Tokyo-Kyoto, Japan, 1988: 121–126.
25. Flores L, Alcocer SM. Calculated response of confined masonry structures. *11th World Conference on Earthquake Engineering*, Acapulco, Mexico, 1996; paper no. 1830.
26. Riahi Z, Elwood KJ, Alcocer SM. Backbone model for confined masonry walls for performance-based seismic design. *Journal of Structural Engineering* 2009; **135**(6):644–654.
27. Tomažević M, Klemenc I. Verification of seismic resistance of confined masonry buildings. *Earthquake Engineering & Structural Dynamics* 1997; **26**(10):1073–1088.
28. Lafuente M, Castilla E, Genatios C. Experimental and analytical evaluation of the seismic resistant behaviour of masonry walls. *Masonry International* 1998; **11**(3):80–88.
29. Bourzam A, Goto T, Myiajima M. Shear capacity prediction of confined masonry walls subjected to cyclic lateral loading. *Doboku Gakkai Ronbunshuu A* 2008; **64**(4):692–704.
30. NSPRC, Chinese code for seismic design of buildings (GB50011-2001). National Standard of the People's Republic of China (NSPRC), Ministry of Construction of People's Republic of China, Beijing, China, 2001.
31. Rai DC, Singhal V, Paikara S, Mukherjee D. Sub-paneling of masonry walls using pre-cast RC elements for earthquake resistance. *Earthquake Spectra* 2014; **30**(2):913–937.
32. Timoshenko S, Woinowsky-Krieger S. *Theory of Plates and Shells*, 2. McGraw-hill: New York, 1959.
33. IITK-GSDMA. Proposed draft provisions and commentary on structural use of unreinforced masonry. National Information Center for Earthquake Engineering (NICEE), Indian Institute of Technology Kanpur, Kanpur, India, 2007.
34. Yoshimura K, Kikuchi K, Kuroki M, Nonaka H, Kim KT, Wangdi R, Oshikata A. Experimental study on effect of height of lateral forces, column reinforcement and wall reinforcements on seismic behavior of confined masonry walls. *Proceeding of the 13th World Conference of Earthquake Engineering*, Vancouver, Canada, 2004; paper no. 1870.
35. Riahi Z. Performance-based seismic models for confined masonry walls. *Masters' Thesis*, Department of Civil Engineering, University of British Columbia, Vancouver, 2007.
36. Kuroki M, Kikuchi K, Nonaka H, Shimozaki M. Experimental study on reinforcing methods using extra RC elements for confined masonry walls with openings. *15th World Conference on Earthquake Engineering*, Lisbon, Portugal, September 2012; paper no. 4967

37. Mohammadi M, Nikfar F. Strength and stiffness of masonry-infilled frames with central openings based on experimental results. *Journal of Structural Engineering* 2013; **139**(6):974–984.
38. Al-Chaar G. Evaluating strength and stiffness of unreinforced masonry infill structures. *Rep. No. ERDC/CERL TR-02-1*, U.S. Army Corps of Engineers: Champaign, IL, 2002.
39. New Zealand Society for Earthquake Engineering (NZSEE). Assessment and improvement of the structural performance of buildings in earthquakes, Wellington, New Zealand, 2006.
40. Mondal G, Jain SK. Lateral stiffness of masonry infilled reinforced concrete (RC) frames with central opening. *Earthquake Spectra* 2008; **24**(3):701–723.
41. Tasnimi AA, Mohebkah A. Investigation on the behavior of brick-infilled steel frames with openings, experimental and analytical approaches. *Engineering Structures* 2011; **33**(3):968–980.
42. Asteris PG, Chrysostomou CZ, Giannopoulos IP, Smyrou E. Masonry infilled reinforced concrete frames with openings. *3rd International Conference on Computational Methods in Structural Dynamics and Earthquake Engineering (COMPdyn)*, European Community on Computational Methods in Applied Sciences, Barcelona, Spain, 2011.